energies

Article

The Strike-Slip Fault Effects on the Ediacaran Carbonate Tight Reservoirs in the Central Sichuan Basin, China

Bing He [1,2], Yicheng Liu [2], Chen Qiu [1], Yun Liu [2], Chen Su [2], Qingsong Tang [2,*], Weizhen Tian [1] and Guanghui Wu [1,*]

1 School of Geoscience and Technology, Southwest Petroleum University, Chengdu 610500, China; hbing1@petrochina.com.cn (B.H.); qiuchen0419@163.com (C.Q.); 18244272539@163.com (W.T.)
2 PetroChina Southwest Oil & Gasfield Company, Chengdu 610051, China; liuyicng@petrochina.com.cn (Y.L.); liuyun1994@petrochina.com.cn (Y.L.); sc0825@petrochina.com.cn (C.S.)
* Correspondence: tangqingsong2008@petrochina.com.cn (Q.T.); wugh@swpu.edu.cn (G.W.)

Abstract: The largest Precambrian gas field in China has been found in the central Sichuan Basin. It is assumed as a mound-shoal microfacies-controlled dolomite reservoir. Recently, a large strike-slip fault system has been identified in the gas field that needs further study of its effect on the Ediacaran reservoirs for highly efficient exploitation of the gas field. For this contribution, we study the matrix reservoir and fractured reservoir along the strike-slip fault damage zones by the cores, FMI (Formation MicroScanner Image) and logging interpretation data, seismic description and production data. It has shown that the matrix reservoir is tight (porosity less than 3%, permeability less than 0.5 mD) that cannot support economical production by conventional exploitation technology in the deep subsurface. On the other hand, the porosity and permeability of the Ediacaran fractured reservoirs could be increased more than one time and 1–3 orders of magnitude. Except for a few localized fracture zones, the fracture elements and fractured reservoirs show a paw-law distribution with the distance to the fault core. Furthermore, the fault effect is more favorable for the increase in the porosity and permeability of the matrix reservoir in the intraplatform than in the platform margin. The overlapping of mound-shoal microfacies, fracturing and karstification could result in large-scale “sweet spots” of the fractured reservoirs in the fault damage zone. The “sweet spot” of fractured reservoir in the fault damage zone is a new favorable exploitation target in the deep central Sichuan Basin.

Keywords: Precambrian; fault damage zone; tight matrix reservoir; fractured reservoir; distribution; Sichuan Basin

check for updates

Citation: He, B.; Liu, Y.; Qiu, C.; Liu, Y.; Su, C.; Tang, Q.; Tian, W.; Wu, G. The Strike-Slip Fault Effects on the Ediacaran Carbonate Tight Reservoirs in the Central Sichuan Basin, China. *Energies* **2023**, *16*, 4041. https://doi.org/10.3390/en16104041

Academic Editor: Jianchao Cai

Received: 8 December 2022
Revised: 18 April 2023
Accepted: 9 May 2023
Published: 11 May 2023

1. Introduction

The deep (>4500 m) carbonate oil/gas resource has become one major exploitation frontier on Earth [1–3]. Due to the deep carbonate reservoir generally having low porosity and permeability, fractured reservoir plays a more significant role in oil/gas exploitation in the deep subsurface [1–6]. Generally, the fracture effect can enhance permeability by more than 1–2 orders of magnitude and increase porosity by over 20% in the deep tight reservoirs along the fault damage zones [1–7]. Particularly, the fracture-related dissolution could result in large fracture-cave reservoir, which could be the “sweet spot” reservoir in deep oil/gas exploitation [2,6–8]. The fracture elements and fractured reservoirs generally present a power–law relationship with distance to the fault core [6,9,10]. Whereas the fractured reservoir is characterized by a strong heterogeneity in the fault damage zones during the long diagenetic history [2,3,6], which could be related to the complicated fracturing, fracture network, lithology and diagenesis along the fault damage zone [6,9–12]. Although fracture can increase the reservoir permeability to a large extent, it is still an enigma in evaluating the increased quantity of the porosity and permeability by fracturing in the deep subsurface. The fractured reservoirs were generally predicted and identified by seismic methods in the deep subsurface [2,3,13–16]. In addition, FMI (Formation MicroScanner Image) and logging data are widely used to evaluate the fractured reservoir in the boreholes [6,17–20]. However, there are generally tremendous challenges in the identification of the strong heterogeneous small-scall reservoirs in the deep subsurface. It is still ambiguous whether there are large-scale fractured reservoirs along the small strike-slip fault zone in the deep subsurface [2,3]. In this context, the integration of geological, logging and seismic methods is important in the description and evaluation of the fractured reservoirs in the deep oil/gas exploitation.

Recently, the largest Precambrian gas field in China has been found in the central Sichuan Basin [21]. The Ediacaran dolomite reservoir has generally been attributed to the mound-shoal facies related reservoir in a carbonate platform and superimposed by karstification at the end of the Ediacaran [21–23]. The matrix pore-type reservoir developed well in the high-energic mound-shoal bodies and was helpful for the development of the meteoric dissolution porosity [23,24]. Whereas most porosity in the Ediacaran reservoir is of secondary dissolution pores with strong heterogeneity [21–24]. In the reservoir development stage, more wells penetrated the matrix reservoirs presenting extremely low porosity-permeability and low production [3,25]. Generally, the conventional exploitation technology could not obtain high gas production from the matrix reservoirs. The technologies of reservoir modeling and seismic prediction, the horizontal well drilling and large-scale fracturing have been used in the matrix reservoirs [25]. Although the gas production can be increased to some extent, many low-production wells also occur in the deep matrix reservoirs. Recently, a large strike-slip fault system has been found in the central Sichuan Basin [26,27]. The studies suggest that the strike-slip fault system has affected the diversity of the Ediacaran microfacies [28] and the source–reservoir connection, reservoir improvement, gas accumulation and high production in the deep carbonate reservoirs [27]. The seismic illumination method has been used to describe the fractured reservoir [3]. However, there is still a big challenge in the seismic description of the fractured reservoir [3], and little geological and logging data has been used to characterize the fractured reservoirs in fault damage zones. Subsequently, it is still ambiguous on the fault effect on the carbonate reservoir, which has hampered the exploitation deployment in the deep Ediacaran reservoirs.

For this contribution, we characterize the fractured reservoirs in the Ayue gas field by cores and FMI data, and present the statistical data of porosity and permeability by logging interpretation in the fault damage zone. Furthermore, we analyze the distribution of the fractured reservoirs across the fault zone and in different sedimentary facies. Finally, we discuss the fracture effects on the increase in the matrix reservoirs and distribution of the fractured reservoirs in the deep Ediacaran carbonate.

2. Geological and Exploitation Background

The Sichuan intracratonic basin in China is characterized by multiple tectonic-sedimentary evolutions [29,30]. The Ediacaran rift sequence unconformably developed on the metamorphic basement (Figure 1). The Upper Ediacaran carbonate platform developed through the basin and consisted of two sets of thin shales. The Lower Cambrian shales are unconformably overlain on the Ediacaran carbonate rocks, which is a better regional source rock and cap rock [30]. A carbonate platform was inherited and developed during the Cambrian–Ordovician. The central uplift initiated from the end of the Ordovician to the early Permian, which resulted in the loss of the Silurian–Carboniferous strata [29]. The carbonate succession deposited from the Permian to the middle Triassic again and was unconformably overlain by the late Triassic to Cretaceous continental strata. Large amounts of sedimentary rocks have been denudated and subsequently formed unconformities by the Indosinian and Yanshan movements [29,30]. During the Himalayan movement, the thrust-fold structures formed around the basinal margins [29]. Regardless of complicated tectonic evolution, the central paleo-uplift has inherited development in the central basin [29,30].

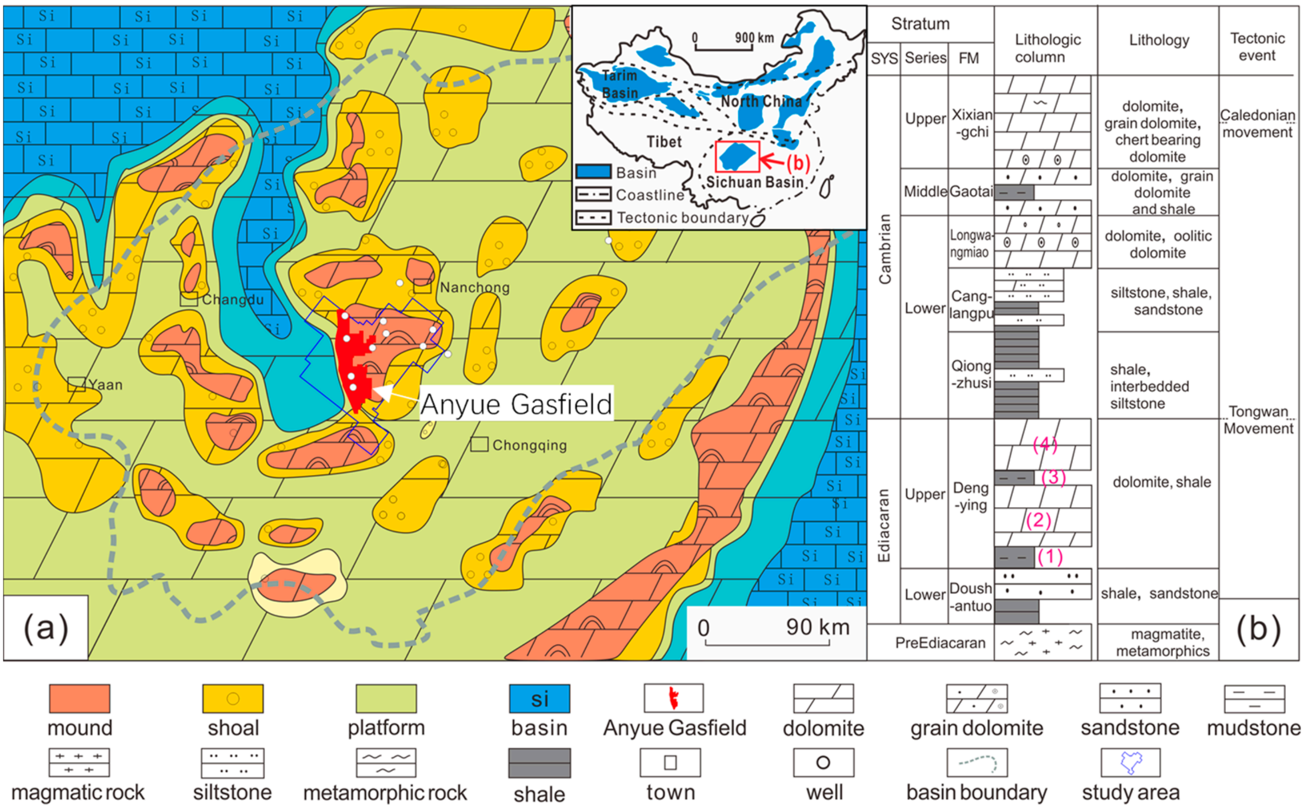

Figure 1. (**a**) The paleogeographic map of the Ediacaran Dengying Formation (schematic map showing the location of the Sichuan Basin in China) and (**b**) the stratigraphic column of the Ediacaran–Cambrian in the Sichuan Basin ((1)–(4): four members of Dengying Formation; SYS: system; FM: formation; after references [3]).

The Anyue gas field is located in the central uplift with an N–S-trending Ediacaran carbonate platform developed to the western rift trough (Figure 1) [31]. The major production zone is the fourth member of the Dengying Formation at the top of the Ediacaran [25]. The Ediacaran mound-shoal microfacies developed widely along the platform margin and interior, which led to widespread matrix porosity [21–24]. At the end of the Ediacaran, a Precambrian unconformity formed in the central uplift [23]. The karstic dissolution pore-vugs developed along the weathering crust with a depth of 200 m [21–23]. The carbonate reservoirs are characterized by multiple vertical layers with varied thicknesses in the range of 1~40 m. The reservoir is generally composed of microbial, interparticle dissolution pores and vugs [21–24]. The reservoir space of pore, vug and fracture are heterogeneous in the plane and vertical direction. In addition, they present varied porosity and permeability at 2–6% and 0.01–5 mD, respectively. Most well productions are variable in a large range of (1–20) $\times$ 10^4 m^3/d [3]. These suggest that the Ediacaran reservoir is characterized by multi-porosity, intense heterogeneity and variable production. The seismic description and horizontal drilling have been used to increase the gas production in the mound-shoal reservoirs [25]. Whereas there are still many low-production wells that constrain the economic exploitation of the deep ancient reservoirs.

3. Data and Methods

We collected the static and dynamic data from 60 production wells in the Ediacaran carbonates. Due to sparse cores being available for fractured reservoir characterization, we carried out FMI (Formation MicroScanner Image) processing and interpretation of the fractured reservoirs in 21 wells. FMI is a kind of borehole image logging technology from Schlumberger that has 4 arms and 4 pads with 24 electrodes on each pad and a total of 192 electrodes [19]. The radial micro-resistivity measurement has a vertical sampling of

0.25 cm and a vertical resolution of 0.5 cm, which are frequently used to detect the type, aperture and orientation of small-scale fractures [17–20]. Considering that the fracture elements correlate with the distance from the fault core [9,10], we compiled core and FMI data of fracture frequency, orientation and fault rock to describe the fractured reservoirs. Fracture frequency (density) was determined by the fracture number in a specified logging length [10]. In addition, we collected physical properties from cores and logging data to analyze the porosity and permeability of the fractured reservoirs (same with references [6,19]). We use CIFLog2.0 software to interpret these logging parameters of the fractured reservoirs (see the detailed method in reference [20]). These measurements allow a detailed analysis of fractured reservoirs along the fault damage zone [6].

In the Anyue gas field, it is hard to identify the small vertical displacement (<30 m) of the strike-slip fault in the seismic sections [27]. Therefore, recent pre-stack time and depth migration processing has been carried out in the 7066 km^2 3D area [3]. These high-resolution seismic data are favorable for the identification of the strike-slip fault in the deep subsurface. The coherence, maximum likelihood and steerable pyramid attributes are used for the mapping of the strike-slip faults [3] and are helpful for the description of the fault damage zones [3]. Together with these methods and data, we describe the fractured reservoirs and analysis the fracture effect on the carbonate reservoirs.

4. Fractured Reservoirs

4.1. Distribution of the Strike-Slip Faults

By the identification and interpretation of strike-slip faults, 22 large strike-slip fault zones with a total length of 720 km have been found in the Anyue gas field (Figure 2a). Most strike-slip faults are NWW-trending, which is consistent with previous studies [27]. Some small NE-trending strike-slip faults have been identified by new data, which could have been across the study area. The strike-slip faults developed in the Ediacaran are characterized by multiple isolate soft-linked segments. Most segments form en échelon or oblique assemblages. Generally, these isolate segments suggest the unmature characteristic of a strike-slip fault zone. Some horsts and a few minimum pull-apart grabens developed in the overlap zones. The horsetail structures developed in the eastern fault tips suggest the eastward propagation of the strike-slip zone.

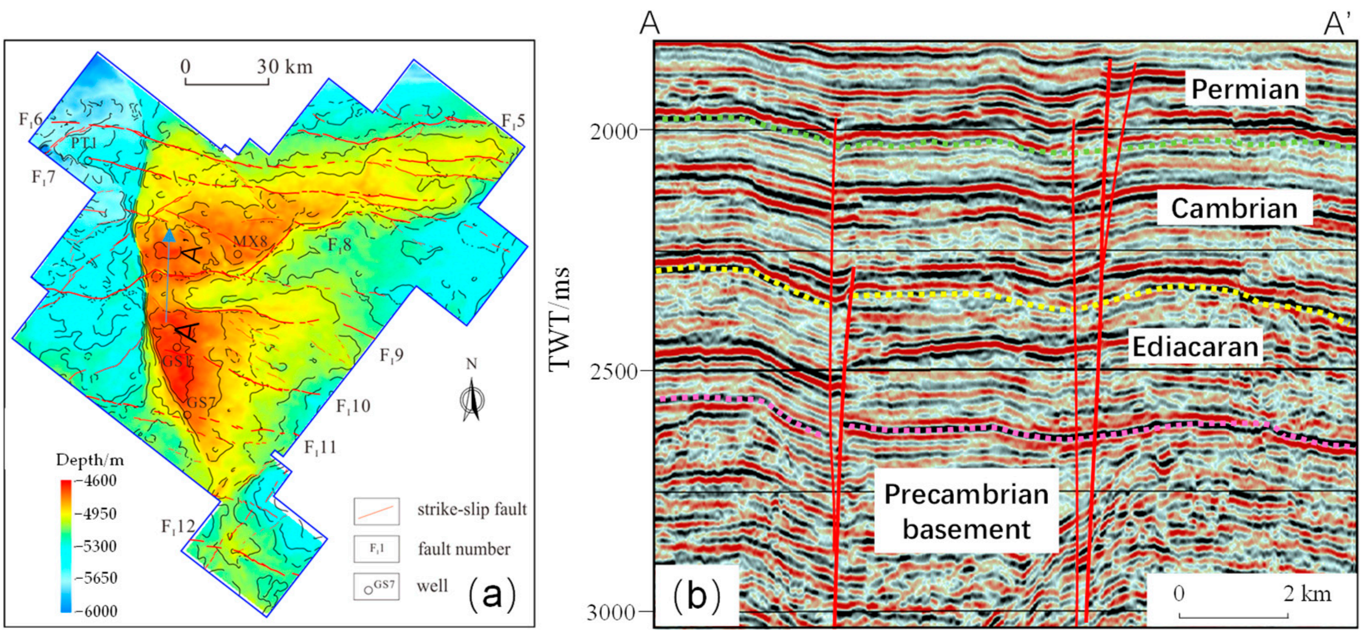

Figure 2. (**a**) Distribution of strike-slip faults and (**b**) typical seismic section in the Anyue gas field. The order of the strike-slip faults is after their length and displacement (TWT: two-way travel time).

The strike-slip faults present vertical linear fault lines and some flower structures in the seismic section (Figure 2b). It noted that the vertical displacement is generally less than 30 m. The relatively small displacement has resulted in an ambiguous fault surface. In this context, the fault zone generally presents a chaotic, discontinuous seismic reflection. The strike-slip faults developed in the Ediacaran and propagated to the Permian. The multiple flower structures that developed in the Ediacaran-Cambrian, Permian and Triassic-Jurassic, suggest multiple inherited growth of the strike-slip fault zone. Considering some faults terminated at the top of the Ediacaran and the unconformity under the Cambrian, it can be inferred that there was a strike-slip fault activity before the Cambrian deposition. This is consistent with the major fault activity at the end of the Ediacaran [27].

In the illumination attribute (Figure 3), there is a distinct image of the boundary of the fault damage zone. Although it is hard to identify the fault surface, the center of the intense damage zone could indicate the fault core. Generally, the seismic attribute suggests symmetrical damage zones on both sides of the fault core. The stronger intensity of the illumination attribute suggests the intense damage zone. The width of the fault damage zone generally varies in the range of 100–500 m and can be more than 1 km in the fault overlap zones. This is consistent with the fractured reservoirs by logging data. In addition, the attribute can also be used to describe the fractured reservoirs. These suggest that there is a relatively wide fault damage zone in the small strike-slip fault zone.

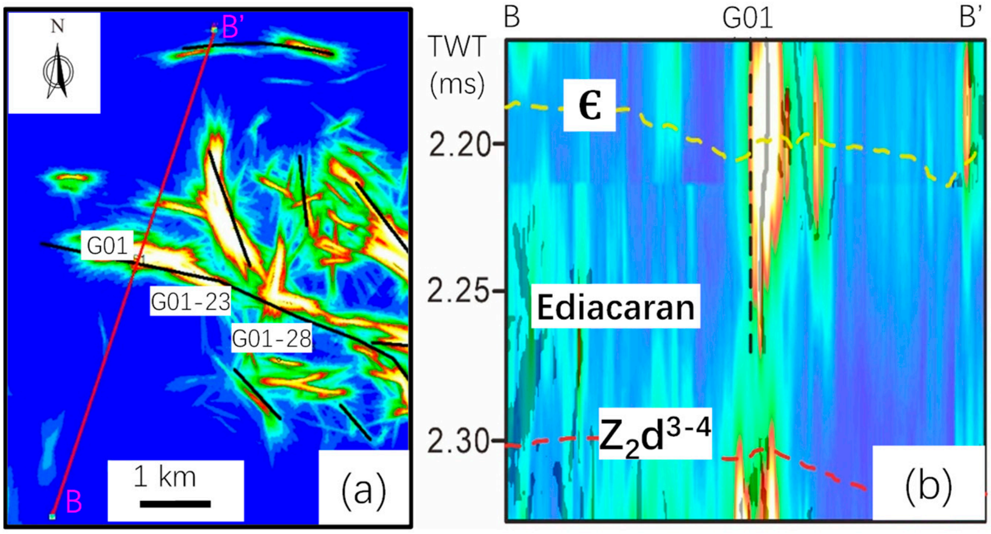

Figure 3. Illumination attribute showing fault damage zone in plane (**a**) (the black lines showing the fault lines by seismic interpretation) and section (**b**) in well G1 area (Є: bottom of the Cambrian; $Z_2d^{3–4}$: the third-fourth section of the Dengying Formation in the Upper Ediacaran; the green-yellow blocks showing the fault damage zones).

4.2. Fractured Reservoirs in Borehole

The Ediacaran dolomite reservoirs are mainly mound-shoal facies in a broad platform [23,24], having a thickness of more than 500 m in the central Sichuan Basin (Figure 2). However, most primary porosity in the Ediacaran reservoirs has been occluded to show tight dolomites (Figure 4a). Through investigation of the cores and thin sections, more than 80% of porosity is secondary dissolution vug (diameter between 2 and 100 mm) (Figure 4). Further, the fracture and its related dissolution porosity are common in the cores and image logging data (Figure 4c,d). A few wells in the fault zone presented fracture-cave reservoirs (cave diameter of more than 100 mm).

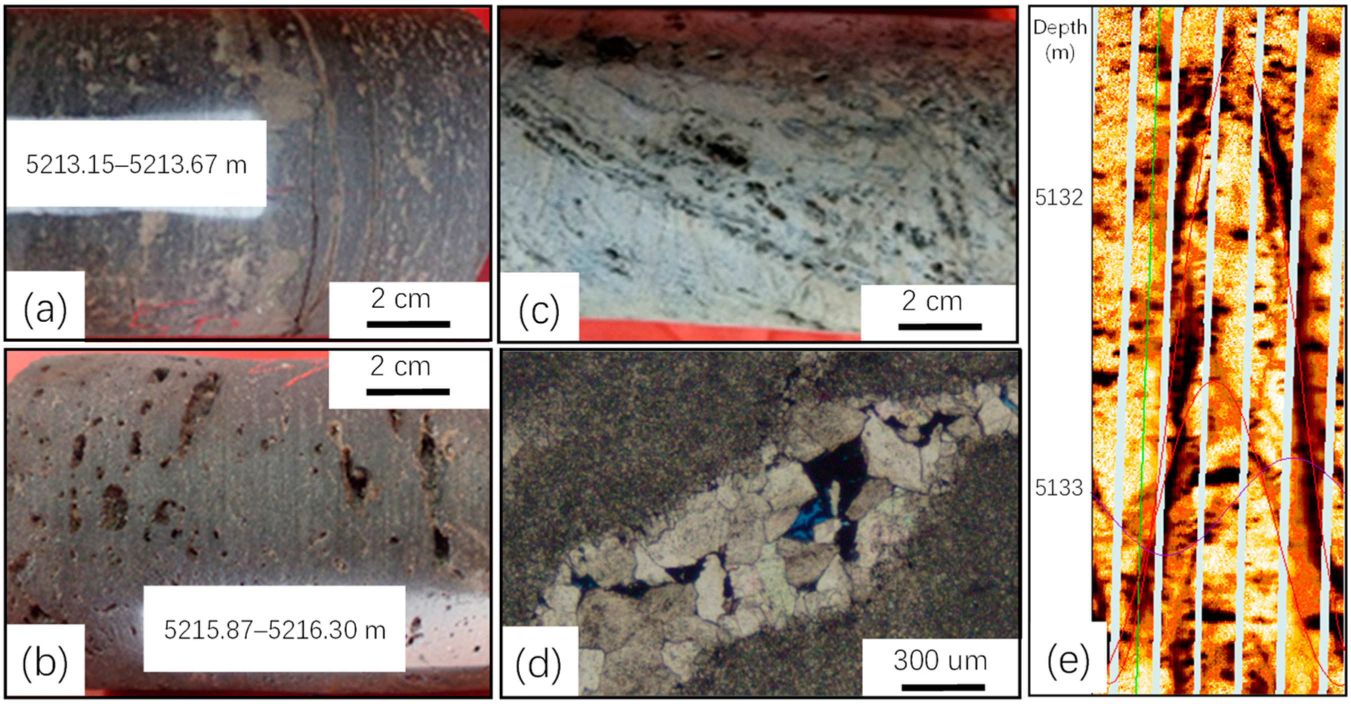

Figure 4. Photographs of the Ediacaran carbonate reservoirs. (**a**) tight dolomite in the reservoir, core; (**b**) horizontal dissolution vugs, core; (**c**) dissolution vugs along the high-angle fractures, core; (**d**) dissolution pores (dark and blue blocks in the granular cements) and dolomite cements along fractures, thin section; (**e**) FMI image showing fractures and dissolution pores along the fractures (the red hyperbolic curve showing fracture, the dark spots showing the dissolution vugs).

The matrix porosity developed well in the Ediacaran mound-shoal bodies [21–24]. However, the porosity is mainly of intercrystalline dissolution pores (Figure 4b). The dissolved pores and vugs are common in the grainstones of the mound-shoal facies. The primary porosity has almost been lost by multiple cementations during the long process of diagenesis. Generally, the porosity formed at the early stage had intense cementation (Figure 4b). Subsequently, the Ediacaran matrix porosity and the permeability are almost less than 3% and 0.5 mD, respectively. Even in the grainstones, there are also very low porosity and permeability with dissolution pores. Although horizontal drilling and large-scale fracturing have been implemented in the matrix reservoirs, the matrix reservoir lacking fractures generally presented low gas production.

Through cores and FMI image investigation, fractures developed at high angles and narrow apertures in the fractured reservoirs. The fracture porosity in the carbonate reservoir is almost lower than 0.1%, whereas the permeability can increase by 1–3 orders of magnitude (Figure 5). Most core plug samples with fractures present permeability of more than 5 mD, but the matrix samples show lower than 0.5 mD. Moreover, the dissolution pores developed well along the fractures to show porosity up to 3–8% (Figure 4c,d). It noted that the micro-throat's radius is less than 0.1 μm in matrix reservoirs but more than 5 μm in fractured reservoirs. Generally, high production well penetrated into fractured reservoirs with mud leakage and drilling break. These porosities form two kinds of reservoirs of tight matrix reservoirs and high permeable fractured reservoirs. Although the porosity is less than 3% and the permeability is less than 0.5 mD in the matrix reservoirs, the permeability can be increased by 1–3 orders of magnitude and the porosity can be increased more than 2 times in the fractured reservoirs (Figure 5). Furthermore, the Ediacaran reservoirs present intense heterogeneity with varied physical properties of reservoirs in the fault damage zones. These heterogeneous fractured reservoirs are quite different from the porous carbonate reservoirs in Meso–Cenozoic.

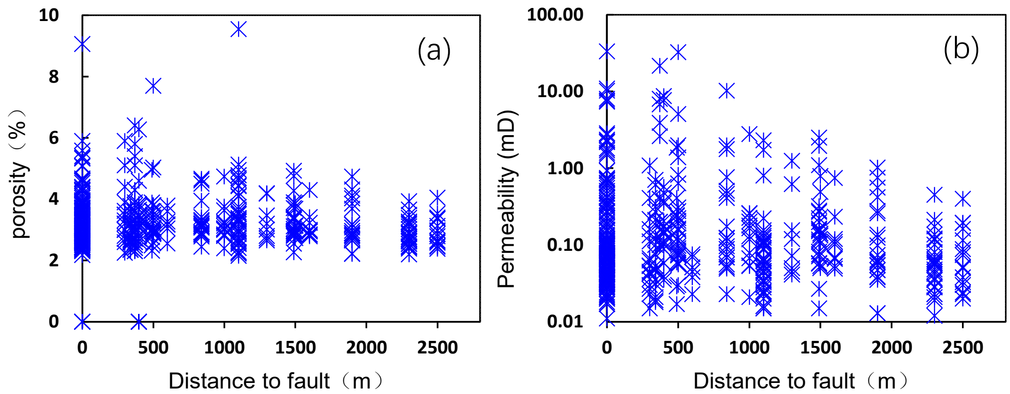

Figure 5. Porosity (**a**) and permeability (**b**) vs. distance to fault in the Ediacaran reservoirs.

4.3. Fractured Reservoirs across the Fault Damage Zone

Due to fewer cores obtained in a fault damage zone, we analyzed the fractured reservoirs by the FMI data processing and interpretation (Figure 6). Constrained by the seismic attributes, most fractured intervals developed within 800 m of the fault cores.

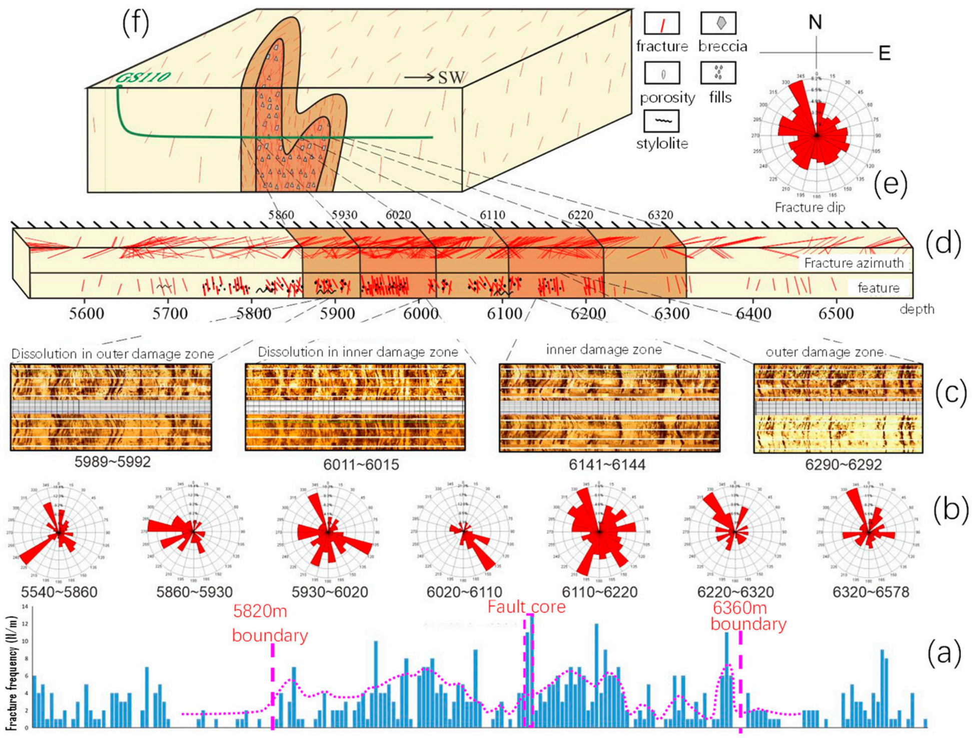

Figure 6. The Ediacaran fractured reservoir across a strike-slip fault zone in a horizontal well ((**a**): the fracture frequency; (**b**): the diagram showing the fracture strike; (**c**): FMI images of the fault damage zone; (**d**): the fracture distribution model in the borehole; (**e**): the rose diagram showing the fracture dips; (**f**): 3D model of the fault damage zone).

Fractures in fault zones are mainly in narrow openings (<1 mm), but some wider fractures exist near the fault cores. Some fractures are filled with carbonate, argillaceous or arenaceous. The unfilled and partially filled fractures represent about 20–70% of the total fractures. The total filled fractures generally have low fracture frequency. The fractures developed and changed frequently in the fault damage zone. In fractured intervals, the fracture frequency is more than 4/m, particularly in the inner damage zones. Whereas the fracture frequency in country rocks is generally less than 1/m. Except for some abnormal data, the fracture frequency shows a decreasing trend with distance to the fault core

(Figure 6). Generally, there is a much higher fracture frequency in the inner damage zone rather than fewer high fracture frequencies in the outer damage zone. The fracture frequency varies across the fault damage zone, which could be disturbed by secondary faults that are hard to be imaged with the seismic data. It is noteworthy that some fracture zones in the country rocks could lead to localized high fracture frequency, which might be related to the small secondary faults that have not been imaged by the seismic data.

Further, the porosity and permeability of the fractured reservoirs are varied in a large range across the strike-slip fault damage zone. In the horizontal borehole (Figure 7), the logging porosity and permeability in the country rocks are generally less than 2% and less than 0.1 mD, respectively. Some abnormal permeability and porosity values are related to the localized fracture zones and dissolution, respectively. The porosity and permeability in the fault damage zone are increasing from 2% to 5% and from 0.01 mD to 1 mD. Particularly, some much higher permeability values have occurred in the localized fracture zones. The porosity and permeability of the fractured reservoirs are generally enhanced more than 2–4 times and 1–3 orders of magnitude across the fault zone. In addition, the porosity and permeability values are relatively higher in the inner zone than in the outer zone. In this way, the petrophysical properties are variable across the fault damage zone that could be used to identify the fault boundaries. These suggest that the fracturing in the fault damage zone could enhance the reservoirs to a large extent. The porosity and permeability values show a negative power-law relationship with the distance to the fault core (Figure 7). Most of the high permeability values of more than 5 mD are within the fault damage zone. Of course, porosity and permeability show a large scatter within the fault damage zone. This can correlate with the fracture frequency in the fault damage zone (Figure 6).

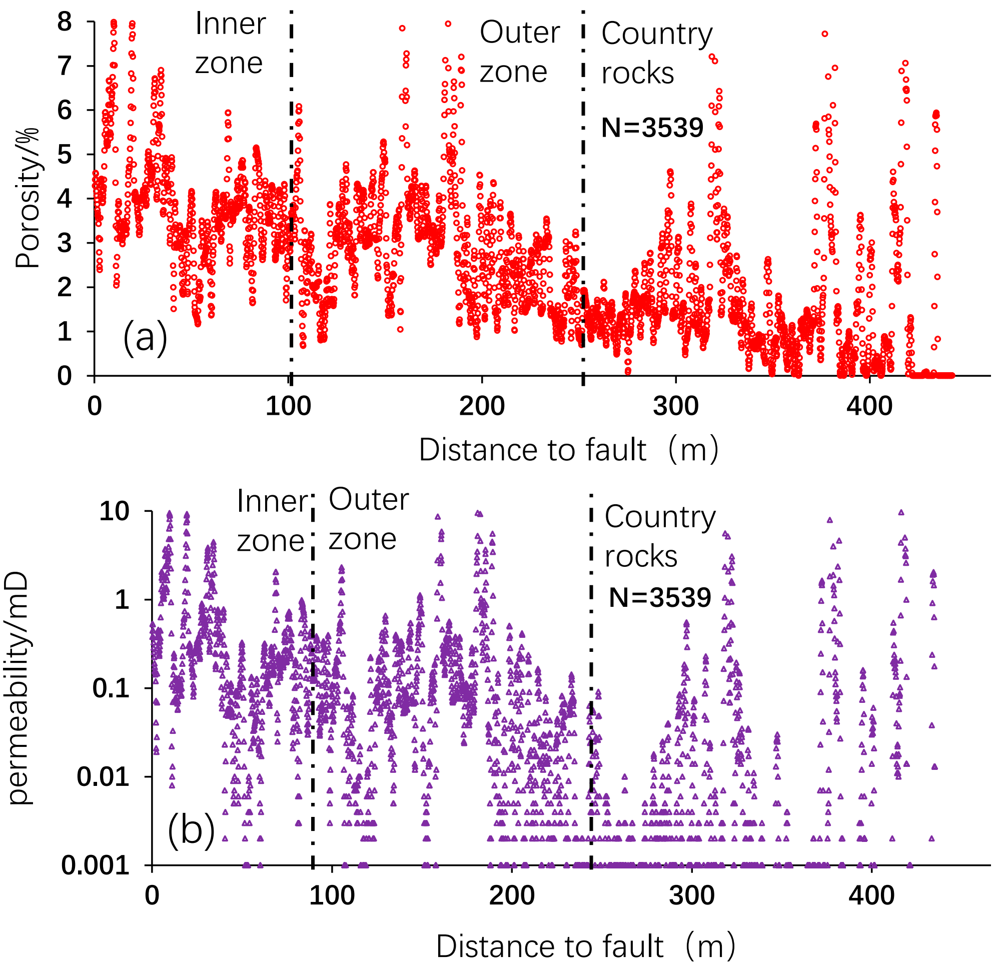

Figure 7. The porosity (**a**) and permeability (**b**) across a strike-slip fault zone in a well (the abnormal high porosity and permeability values in the country rocks are related with localized fracture zone).

5. Discussion

5.1. Fracture Effect on the Ediacaran Reservoirs

Previous studies suggest that the mound-shoal controlled reservoirs developed well in the deep Ediacaran carbonate platform margin and interior, and formed large areas of dolomite pore-type reservoirs [21,22]. Recently, it has been suggested that the syngenetic karstification is the main controlling factor for the development of carbonate reservoirs [23]. Even so, the Ediacaran matrix reservoir is mainly of low porosity-permeability (<4% and <1 mD, respectively) (Figures 5 and 7). This is slightly higher than the Ordovician limestone reservoir in the Tarim Basin [2,6,31–33] and comparable to the global deep tight reservoir [34]. Previous studies have argued that the Ediacaran reservoirs had experienced long diagenesis and occluded most primary porosity to show secondary dissolution porosity [21–24]. Through the new strike-slip fault mapping, the locations of most high-production wells fall into the strike-slip fault zones, which suggests that the fracturing had an important effect on the development of secondary porosity and the "sweet spot" of the fractured reservoir.

Statistical data in this study suggest that the fracture network developed along fault damage zones could be more than 500 m in width (Figures 3, 5 and 6). The width of the fault damage zones is more than that with similar displacement in other places [9]. Although the boundary of the fault damage zone by seismic description needs further study [3,35], these data suggest that the small strike-slip faults could have resulted in a wide fault damage zone. Regardless of low fracture porosity (<0.1%) in the dolomite reservoir, the secondary dissolved porosity along the fracture could increase more than 2 times along the fault damage zone. This suggests that the fault damage zone is more favorable for the development of the karstic dissolution of vugs (Figure 4c–e). In the carbonate fault damage zone, the increased porosity of the fracture-vug and fracture-cave reservoirs could be correlated with the fracture-cave reservoirs in the Tarim Basin [2,6,31]. Seismic reservoir description shows that the fractured reservoirs developed generally within 500 m in the fault damage zones, particularly in the inner damage zone (Figure 3). Whereas some "sweet spots" of fracture-vug reservoirs could occur in the outer damage zone and beyond the fault damage zone. These could be possibly correlated to the passage effect of the fault zone that transports the fluid to the country rocks for dissolution.

Furthermore, fracturing has controlled the permeability of the tight Ediacaran reservoirs. This is consistent with the fault effect on the permeability in other places [1–6]. The permeability from plug cores of the matrix reservoir is generally varied in the range of 0.005–1 mD but varied in the range of 0.1–100 mD in fractured samples, which can be increased by 2–3 orders of magnitude. However, the permeability of the fractured reservoir may be increased by 1–2 orders of magnitude from the logging data. This suggests that there is a relatively weak connectivity of the fracture network that led to the relatively lower permeability of the reservoirs.

Consequently, the strike-slip fault process can lead to a wide fault damage zone and subsequent high permeable fracture network that is favorable for the development of the dissolution porosity.

5.2. Reservoirs in Different Sedimentary Facies Belts

It has shown that the E-W trending syn-sedimentary strike-slip fault activity could have affected the diversity of the Ediacaran sedimentary microfacies in the carbonate platform [28]. The fault effects on the paleogeography could have led to the varied distribution of the mound-shoal microfacies and subsequent varied reservoirs along and across the strike-slip fault zones. In this way, the strike-slip faults have an important effect on the diversity of the sedimentary facies-controlled reservoirs. This can also be correlated with the intense heterogeneity of the Ediacaran reservoirs and is similar to the intracratonic strike-slip faults in the Tarim Basin [6,10,36].

In the low-energy intraplatform, the strike-slip fault activity had a distinct effect in increasing the permeability and porosity of the Ediacaran reservoirs. By core and well logging interpretation, most values of the porosity (<2%) and permeability (<0.2 mD) of the matrix reservoirs are consistent with the tight reservoirs in other places [6,34]. Whereas the fractures developed well in a fault damage zone that could increase the porosity and permeability more than 2 times and 2 orders of magnitude, respectively. The high-production wells are close to the fault cores within 500 m and penetrated "sweet spots" of fractured reservoirs. These high-production wells are closely related to strike-slip fault damage zones, which controlled a high permeable fracture network and subsequent dissolution passage. The gas production could increase more than 2–5 times in the fractured reservoirs than in the tight matrix reservoirs in the intraplatform. It noted that many high-production wells in the strike-slip fault damage zones present quick production decline.

The intraplatform shoals developed behind the weak-rimmed platform margin [21–24]. It has been argued that some intraplatform shoals along the strike-slip fault zones are closely related to the positive landforms that resulted from the fracture activity at the end of the Ediacaran [28]. In this way, the fracturing could lead to a fracture network and affect the karstification in the intraplatform shoals. The porosity of the intraplatform shoals in this area is generally less than 3%, but the porosity of the fractured shoals could be increased more than one time by fracturing and dissolution overlapping with the intraplatform shoals with high matrix porosity. At the same time, the reservoir permeability has increased significantly more than 1–2 orders of magnitude. The gas production in the fractured intraplatform shoals could be more than two times than that of the adjacent fractured reservoirs at the outside of the shoals. In addition, there are more stable gas production wells in the intraplatform shoals. This suggests that both the fracture and microfacies have been affected by the Ediacaran reservoirs.

In the rimmed platform margin, the Ediacaran high-energy mound-shoal bodies developed and suffered intense karstification before the Cambrian deposition [21–24]. The matrix porosity and permeability of the mound-shoal reservoirs are generally in the range of 2–6% and 0.02–1 mD, respectively. It is generally assumed that the fractures had no significant effect on the reservoirs [21–24]. Whereas most high-production wells fall into the strike-slip fault zones by recent seismic descriptions of the Ediacaran fault damage zones (Figure 3). This is consistent with the logging interpretation. The production data suggest that higher permeable reservoirs are closely related to fractures that also could increase the permeability of more than 1 order of magnitude. In addition, the porosity of the mound-shoals could increase by more than 50% in the fractured reservoirs. In this context, the carbonate reservoirs were controlled by the high-energy mound-shoal microfacies along the platform margin and increased by the strike-slip fracturing. Considering that the high-energy mound-shoal reservoirs are generally of low porosity (<5%) and low permeability (<2 mD), the fracture network could have a more significant effect on the high gas production. It should be noted that the "sweet spots" of high-production wells generally occurred in the strike-slip fault damage zones. In this way, the relatively higher matrix porosity is significantly improved by the fracturing and related karstification. This is consistent with the Ordovician carbonate platform margin in the central Tarim Basin [35].

Consequently, there are three typical reservoirs of fracture-controlled reservoirs in the low-energic intraplatform, high-energic microfacies and fracturing-controlled reservoirs in the intraplatform shoals, and high-energic microfacies controlled mound-shoal reservoirs overlapped fractured reservoirs along the strike-slip fault zones. The three elements of microfacies, fracturing and dissolution, have controlled the development and distribution of high-quality reservoirs. These processes resulted in the varied fault effects on the different sedimentary rocks and varied reservoirs along the strike-slip fault zones.

6. Conclusions

1. The Ediacaran matrix reservoir (porosity < 3%, permeability < 0.5 mD) is too tight to result in high gas production in the deep Sichuan Basin;
2. The porosity and permeability of the Ediacaran matrix reservoirs could be increased over one time and 1–3 orders of magnitude in the fault damage zone. The fractures, porosity and permeability present an increased trend from the host rocks to the strike-slip fault core, but the localized fracture zones show abnormally high values;
3. The superimposed mound-shoal microfacies, fracturing and karstification in the fault damage zones have led to the varied fault effects on the reservoir petrophysical properties and distribution in different sedimentary microfacies;
4. The "sweet spot" of a fractured reservoir in the strike-slip fault zone could be a major economic exploitation domain in the deep subsurface.

Author Contributions: Conceptualization, B.H. and G.W.; methodology, C.Q. and B.H.; software, C.Q. and W.T.; investigation, B.H. and G.W.; data curation, Y.L. (Yun Liu) and Y.L. (Yicheng Liu); writing, G.W. and Y.L. (Yicheng Liu); visualization, C.S. and W.T.; supervision, Q.T. and G.W.; funding acquisition, B.H. and Q.T. All authors have read and agreed to the published version of the manuscript.

Funding: The Science and Technology Cooperation Project of the CNPC-SWPU Innovation Alliance (2020CX010101) and the National Natural Science Foundation of China (41972121).

Data Availability Statement: Not applicable.

Acknowledgments: The authors are grateful to the editors and reviewers for their comments regarding manuscript improvement. We also thank Wei Xu, Bingshan Ma, Wenjun Luo and Puwei He for their help in the data process.

Conflicts of Interest: The authors declare no conflict of interest.

References

1. Sun, L.D.; Zou, C.N.; Zhu, R.K.; Zhang, Y.H.; Zhang, S.C.; Zhang, B.M.; Zhu, G.Y.; Gao, Z.Y. Formation, distribution and potential of deep hydrocarbon resources in China. *Pet. Explor. Dev.* **2013**, *40*, 687–695. [CrossRef]
2. Wang, Q.H.; Zhang, Y.T.; Xie, Z.; Zhao, Y.W.; Zhang, C.; Sun, C.; Wu, G.H. The Advance and challenge of seismic technique on the ultra-deep carbonate reservoir exploitation in the Tarim Basin, Western China. *Energies* **2022**, *15*, 7653. [CrossRef]
3. He, X.; Guo, G.; Tang, Q.; Wu, G.; Xu, W.; Ma, B.; Huang, T.; Tian, W. The advances and challenges of the Ediacaran fractured reservoir development in the central Sichuan Basin, China. *Energies* **2022**, *15*, 8137. [CrossRef]
4. Spencer, C.W. Review of characteristics of low-permeability gas reservoirs in Western United States. *AAPG Bull.* **1989**, *73*, 613–629.
5. Garland, J.; Neilson, J.; Laubach, S.E.; Whidden, K.J. Advances in carbonate exploration and reservoir analysis. *Geol. Soc. Lond. Spec. Publ.* **2012**, *370*, 1–15. [CrossRef]
6. Wu, G.H.; Zhao, K.Z.; Qu, H.Z.; Nicola, S.; Zhang, Y.T.; Han, J.F.; Xu, Y.F. Permeability distribution and scaling in multi-stages carbonate damage zones: Insight from strike-slip fault zones in the Tarim Basin, NW China. *Mar. Pet. Geol.* **2020**, *114*, 104208. [CrossRef]
7. Moore, P.J.; Fernández-Ibáñez, F. Non-Matrix Quick Pass: A rapid evaluation method for natural fractures and karst features in core. *Energies* **2022**, *15*, 4347. [CrossRef]
8. Méndez, J.N.; Jin, Q.; González, M.; Zhang, X.D.; Lobo, C.; Boateng, C.D.; Zambrano, M. Fracture characterization and modeling of karsted carbonate reservoirs: A case study in Tahe oilfield, Tarim Basin (Western China). *Mar. Pet. Geol.* **2020**, *112*, 104104. [CrossRef]
9. Torabi, A.; Berg, S.S. Scaling of fault attributes: A review. *Mar. Petrol. Geol.* **2011**, *28*, 1444–1460. [CrossRef]
10. Wu, G.H.; Gao, L.H.; Zhang, Y.T.; Ning, C.Z.; Xie, E. Fracture attributes in reservoir-scale carbonate fault damage zones and implications for damage zone width and growth in the deep subsurface. *J. Struct. Geol.* **2019**, *118*, 181–193. [CrossRef]
11. Afşar, F.; Westphal, H.; Philipp, S.L. How facies and diagenesis affect fracturing of limestone beds and reservoir permeability in limestone–marl alternations. *Mar. Petrol. Geol.* **2014**, *57*, 418–432. [CrossRef]
12. Debenham, N.; Farrell, N.J.C.; Holford, S.P.; King, R.C.; Healy, D. Spatial distribution of micrometre-scale porosity and permeability across the damage zone of a reverse-reactivated normal fault in a tight sandstone: Insights from the Otway Basin, SE Australia. *Basin Res.* **2019**, *31*, 640–658. [CrossRef]
13. Liu, G.P.; Zeng, L.B.; Han, C.Y.; Ostadhassan, M.; Lyu, W.Y.; Wang, Q.Q.; Zhu, J.W.; Hou, F.X. Natural fractures in carbonate basement reservoirs of the Jizhong Sub-Basin, Bohai Bay Basin, China: Key aspects favoring oil production. *Energies* **2020**, *13*, 4635. [CrossRef]

14. Ou, C.H.; Li, C.C.; Huang, S.Y.; Lu, W.T.; Sheng, J.J.; Xiong, H.L. Three-dimensional discrete network modeling of structural fractures based on the geometric restoration of structure surface: Methodology and its application. *J. Pet. Sci. Eng.* **2018**, *161*, 417–426. [CrossRef]
15. Benmadi, M.; Sayantan, G.; Roger, S.; Kurt, M.; Mashhad, F. Practical aspects of upscaling geocellular geological models for reservoir fluid flow simulations: A case study in integrating geology, geophysics, and petroleum engineering multiscale data from the Hunton Group. *Energies* **2020**, *13*, 1604.
16. Wang, R.J.; Yang, J.P.; Chang, L.J.; Zhang, Y.T.; Sun, C.; Wu, G.H.; Bai, B.C. 3D modeling of fracture-cave reservoir from an ultra−depth strike−slip fault−controlled carbonate oilfield in Northwestern China. *Energies* **2022**, *15*, 6415. [CrossRef]
17. Khoshbakht, F.; Azizzadeh, M.; Memarian, H.; Nourozi, G.H.; Moallemi, S.A. Comparison of electrical image log with core in a fractured carbonate reservoir. *J. Pet. Sci. Eng.* **2012**, *86–87*, 289–296. [CrossRef]
18. Guo, R.X.; Zhang, S.N.; Bai, X.L.; Wang, K.; Sun, X.D.; Liu, X.X. Hydrothermal dolomite reservoirs in a fault system and the factors controlling reservoir formation-A case study of Lower Paleozoic carbonate reservoirs in the Gucheng area, Tarim Basin. *Mar. Pet. Geol.* **2020**, *120*, 104506. [CrossRef]
19. Shafiabadi, M.; Kamkar-Rouhani, A.; Sajadi, S.M. Identification of the fractures of carbonate reservoirs and determination of their dips from FMI image logs using Hough transform algorithm. *Oil Gas Sci. Technol.–Rev. IFP Energ. Nouv.* **2021**, *76*, 202101. [CrossRef]
20. Cao, M.; Gao, Z.; Yuan, Y.; Yan, Z.; Zhang, Y. A visualization and analysis method by multi-dimensional crossplots from multi-well heterogeneous data. *Energies* **2022**, *15*, 2575. [CrossRef]
21. Zhou, Z.; Wang, X.Z.; Yin, G.; Yuan, S.S.; Zeng, S.J. Characteristics and genesis of the (Sinian) Dengying Formation reservoir in Central Sichuan, China. *J. Nat. Gas Sci. Eng.* **2016**, *29*, 311–321. [CrossRef]
22. Luo, B.; Yang, Y.M.; Luo, W.J.; Wen, L.; Wang, W.Z.; Chen, K. Controlling factors of Dengying Formation reservoirs in the central Sichuan paleo-uplift. *Petrol. Res.* **2017**, *2*, 54–63. [CrossRef]
23. Zhou, Y.; Yang, F.L.; Jia, Y.L.; Zhou, X.F.; Zhang, C.H. Characteristics and controlling factors of dolomite karst reservoirs of the Sinian Dengying Formation, central Sichuan Basin, southwestern China. *Precambrian Res.* **2020**, *343*, 105708. [CrossRef]
24. Tian, X.W.; Peng, H.L.; Wang, Y.L.; Yang, D.L.; Sun, Y.T.; Zhang, X.H.; Wen, L.; Luo, B.; Hong, H.T.; Wang, W.Z.; et al. Analysis of reservoir difference and controlling factors between the platform margin and the inner area of the fourth member of Sinian Dengying Formation in Anyue Gas Field, central Sichuan. *Nat. Gas Geosci.* **2020**, *31*, 1225–1238.
25. Xie, J. Innovation and practice of the key technologies for the efficient development of the supergiant Anyue gas field. *Nat. Gas Ind. B* **2020**, *7*, 337–347. [CrossRef]
26. Ma, D.B.; Wang, Z.C.; Duan, S.F.; Gao, J.R.; Jiang, Q.C.; Jiang, H.; Zeng, F.Y.; Lu, W.H. Structural characteristics of strike slip faults and significance of natural gas accumulation in Gaoshiti Moxi area, Sichuan Basin. *Pet. Explor. Dev.* **2018**, *45*, 795–805. [CrossRef]
27. Jiao, F.; Yang, Y.; Ran, Q.; Wu, G.; Liang, H. Distribution and gas exploration of the strike–slip faults in the central Sichuan Basin. *Nat. Gas Ind. B* **2021**, *9*, 63–72. [CrossRef]
28. Wen, L.; Ran, Q.; Tian, W.; Liang, H.; Zhong, Y.; Zou, Y.; Su, C.; Wu, G. Strike-slip fault effects on diversity of the Ediacaran Mound-shoal Distribution in the Central Sichuan Intracratonic Basin, China. *Energies* **2022**, *15*, 5910. [CrossRef]
29. He, D.; Li, D.; Zhang, G.; Zhao, L.; Fan, C.; Lu, R.; Wen, Z. Formation and evolution of multi-cycle superposed Sichuan Basin, China. *Chin. J. Geol.* **2011**, *46*, 589–606. (In Chinese with English Abstract)
30. Li, H.K.; Li, Z.Q.; Long, W.; Wan, S.S.; Ding, X.; Wang, S.Z.; Wang, Q.Z. Vertical configuration of Sichuan Basin and its superimposed characteristics of the prototype basin. *J. Chengdu Univ. Technol.* **2019**, *46*, 257–267. (In Chinese with English Abstract)
31. Yang, H.J.; Wu, G.H.; Scarselli, N.; Sun, C.H.; Qing, H.R.; Han, J.F.; Zhang, G.W. Characterization of reservoirs, fluids, and productions from the Ordovician carbonate condensate field in the Tarim Basin, northwestern China. *AAPG Bull.* **2020**, *104*, 1567–1592. [CrossRef]
32. Shen, F.X.; Li, S.Y.; Deng, X.L.; Liu, Z.L.; Guo, P.; Wu, G.H. Application of EOR using water injection in carbonate condensate reservoirs in the Tarim Basin. *Energies* **2022**, *15*, 3881. [CrossRef]
33. Zhu, Y.F.; Zhang, Y.T.; Zhao, X.X.; Xie, Z.; Wu, G.H.; Li, T.; Yang, S.; Kang, P.F. The fault effects on the oil migration in the ultra-deep Fuman Oilfield of the Tarim Basin, NW China. *Energies* **2022**, *15*, 5789. [CrossRef]
34. Nelson, P.H. Pore-throat sizes in sandstones, tight sandstones, and shales. *AAPG Bull.* **2009**, *93*, 329–340. [CrossRef]
35. Zhao, Y.; Wu, G.; Zhang, Y.; Scarselli, N.; Yan, W.; Sun, C.; Han, J. The strike-slip fault effects on tight Ordovician reef-shoal reservoirs in the Central Tarim Basin (NW China). *Energies* **2023**, *16*, 2575. [CrossRef]
36. Luo, X.; Chen, S.; Liu, J.; Li, F.; Feng, L.; Li, S.; Wu, Y.; Wu, G.; Luo, B. The fractured Permian reservoir and its significance in the gas exploitation in the Sichuan Basin, China. *Energies* **2023**, *16*, 1968. [CrossRef]